Molecular Biology of the Cell
Vol. 19, 1548–1560, April 2008

Immortalization of Neural Precursors When Telomerase Is Overexpressed in Embryonal Carcinomas and Stem Cells

Anneke E. Schwob,* Lilly J. Nguyen,* and Karina F. Meiri

Department of Anatomy and Cellular Biology, Tufts University School of Medicine, Boston MA 02111

Submitted November 15, 2006; Revised January 3, 2008; Accepted January 28, 2008
Monitoring Editor: Marianne Bronner-Fraser

The DNA repair enzyme telomerase maintains chromosome stability by ensuring that telomeres regenerate each time the cell divides, protecting chromosome ends. During onset of neuroectodermal differentiation in P19 embryonal carcinoma (EC) cells three independent techniques (Southern blotting, Q-FISH, and Q-PCR) revealed a catastrophic reduction in telomere length in nestin-expressing neuronal precursors even though telomerase activity remained high. Overexpressing telomerase protein (mTERT) prevented telomere collapse and the neuroepithelial precursors produced continued to divide, but deaggregated and died. Addition of FGF-2 prevented deaggregation, protected the precursors from the apoptotic event that normally accompanies onset of terminal neuronal differentiation, allowed them to evade senescence, and enabled completion of morphological differentiation. Similarly, primary embryonic stem (ES) cells overexpressing mTERT also initiated neuroectodermal differentiation efficiently, acquiring markers of neuronal precursors and mature neurons. ES precursors are normally cultured with FGF-2, and overexpression of mTERT alone was sufficient to allow them to evade senescence. However, when FGF-2 was removed in order for differentiation to be completed most neural precursors underwent apoptosis indicating that in ES cells mTERT is not sufficient allow terminal differentiation of ES neural precursors in vitro. The results demonstrate that telomerase can potentiate the transition between pluripotent stem cell and committed neuron in both EC and ES cells.

INTRODUCTION

In theory, stem cells offer unlimited potential for generating replacements for any differentiated neuron lost due to degeneration or destruction. In practice, significant gaps in our knowledge about how stem cell behavior can be optimized critically hamper full exploitation of their therapeutic potential. One significant problem associated with transplantation of stem cells themselves, namely the inability to control outcomes of differentiation in vivo, has led to a search for alternatives such as partially committed downstream intermediates, for example, precursors selective for a compromised neuronal phenotype (Emsley *et al.*, 2005, Zeng and Rao, 2007). However, neural stems/progenitors are not readily available and have a low mitotic index, raising the problem of how to expand these functional intermediates to produce a clinically useful population.

One strategy that has already had some success is to overexpress telomerase in neural precursor cells. Telomerase is a riboprotein DNA repair enzyme that ensures chromosome stability by maintaining the telomeric protection of chromosome ends during cell division (Natesan, 2005). Its activity is high in stem cells, contributing to their ability to avoid the apoptotic crisis that occurs after chromosome damage during replication. In contrast, the down-regulation of telomerase in most differentiated somatic cells leaves telomeres critically short and cells vulnerable to apoptosis and senescence (Sharpless and DePinho, 2004). Given its proposed role in tumorigenicity, telomerase does not seem to be a promising candidate for precursor expansion. Nonetheless, when the rate-limiting catalytic protein subunit TERT (hTERT in humans, mTERT in mice) was overexpressed in a population of "neural stem cells," i.e., committed neural progenitors isolated from human embryonic spinal cord, the cell lines produced expressed markers of committed neuronal precursors and continued to proliferate past 70 population doublings (70 PD) when senescence would normally occur. When one of these lines was transplanted into injured rat spinal cord, it differentiated into functional neurons that survived for long periods without evidence of either proliferating glia or tumors (Roy *et al.*, 2004). Other cell types suggest a noncanonical role for telomerase in stem cell differentiation: In one example, hair stem cells from an mTERT-overexpressing mouse were recruited from their niche and both proliferation and differentiation were potentiated in vivo (Sarin *et al.*, 2005); in another, overexpressing hTERT in endothelial cells produced an immortalized line of differentiated cells (Chang *et al.*, 2005). Surprising conclusions may be drawn from both these studies: first, that ectopic expression of TERT does not interfere with the completion of differentiation in vivo; and second, that its overexpression is not sufficient to induce tumorigenesis. Clearly, it would be convenient to exploit the pluripotency of embryonic stem (ES) cells by expressing mTERT in the undifferentiated population and then initiating differentiation. Constitutive expression of mTERT in undifferentiated ES cells increased cell numbers in vitro because stress-induced apoptosis was inhibited. Moreover differentiation toward the hematopoietic lineage was enhanced (Armstrong *et al.*, 2000, 2005). Whether this is also true for the neuronal lineage is not known.

This article was published online ahead of print in *MBC in Press* (http://www.molbiolcell.org/cgi/doi/10.1091/mbc.E06–11–1013) on February 6, 2008.

* These authors contributed equally to this work.

Address correspondence to: Dr Karina Meiri (karina.meiri@tufts.edu).

The mechanisms underlying potential telomerase effects are not conveniently examined in ES cells in which neural differentiation takes several weeks to proceed to completion (e.g., Bain *et al.*, 1995). A simpler system that retains the salient features of ES cells, including pluripotency, yet can be differentiated in a highly standardized manner and in a manner that allows outcomes of differentiation to be reproducibly quantitated, is the embryonal carcinoma (EC; Hardy *et al.*, 1990). Like ES cells, undifferentiated EC lines can be induced to differentiate into derivatives of each of the germ layers and, if injected into a blastocyst, can contribute to all of the somatic cell lineages in the developing embryo (Andrews *et al.*, 2005). Like ES cells, undifferentiated EC cells do not form tumors when injected into embryos before embryonic day 13 (E13), but also like ES cells, the incidence of tumors increases with the age of the transplant host (Astigiano *et al.*, 2005). Like ES cells, undifferentiated EC cells do not enter replicative senescence because they handle their senescence regulatory pathways like transformed cells rather than somatic cells, i.e., telomerase levels are high but p53 and the E2F/retinoblastoma protein (pRb) pathways are down-regulated (Miura *et al.*, 2004).

Initiating neuroectodermal differentiation of EC cells by adding retinoic acid (RA) and forcing aggregation into "embryoid-like" bodies, synchronizes the population so that progression through the first four cell cycles can be followed directly (Ninomiya *et al.*, 1997). Neuroectodermal differentiation is independent of extrinsic factors and occurs over a limited time span (5 d compared with >15 d in ES cells) with highly reproducible outcomes (McBurney, 1993) that allow direct analysis of gene expression profiles at distinct stages and enable the gene targets of the differentiation process to be identified (Teramoto *et al.*, 2005). Markers of neuronal progenitors are induced during the third cell cycle (Mani *et al.*, 2001). Here we used both EC and ES cells to show that overexpressing mTERT in the pluripotent cells does not impede initiation of neuroectodermal differentiation and allows a population of precursors with enhanced proliferative potential to be expanded. Both EC and ES cells evade senescence; however, only EC cells are able to quantitatively complete differentiation in vitro.

MATERIALS AND METHODS

TAGGG Assay of Telomere Length

For the assessment of telomere length genomic DNA was prepared from postnatal day 19 (P19) cells that were either undifferentiated or that had been treated with retinoic acid to induce neuroectodermal differentiation (see below). Genomic DNA was digested with HinfI and RsaI to release telomeric fragments and then separated on an 8% agarose gel at 50 V/cm. After electrophoresis, DNA was blotted onto Hybond-N+ membrane and detected using the "Telo TAGGG Telomere Length Assay" kit (Roche, Mannheim, Germany) according to manufacturer's instructions. Briefly, telomere DNA were hybridized to a digoxigenin (DIG)-labeled $(TAGGG)_4$ probe specific for telomeric repeats and then incubated with a DIG-specific antibody covalently coupled to alkaline phosphatase. The immobilized probe was visualized by alkaline phosphatase metabolizing CDP-Star, a highly sensitive chemiluminescence substrate. Telomere length was determined by densitometry of the x-ray film according to the instructions in the assay kit.

Quantitative Fluorescence In Situ Hybridization Assay of Telomere Length

Quantitative fluorescence in situ hybridization (Q-FISH) was performed using a Cy-3–labeled peptide nucleic acid (PNA) probe complementary to the mammalian telomere repeat sequence (N-terminus to C-terminus) CCCTAACCCTAACCCTAA with an N-terminal covalently linked Cy3 fluorescent dye (Applied Biosystems, Framingham, MA), according to Meeker *et al.* (2002) and Molenaar *et al.* (2003) as follows: Fixed cells were placed in 0.1 M citrate buffer and steamed (Black and Decker Handy Steamer Plus; Black and Decker, Towson, MD), cooled, and then extracted in PBS-0.1% Tween-20 followed by 0.5 mg/ml protease type VIII (Sigma Chemical, St. Louis, MO). After rinsing in water followed by 95% ethanol and air-drying, 25 μl of the PNA probe (0.3 μg/ml PNA in 70% formamide, 10 mmol/l Tris, pH 7.5, 0.5% blocking reagent; Boehringer Mannheim, Indianapolis, IN) was applied, and denaturation was carried out at 83°C for 4 min. Slides were then hybridized at room temperature for 2 h, washed in 70% formamide, 10 mmol/L Tris, pH 7.5, 0.1% albumin followed by TBS, and then either counterstained with DAPI (250 ng/ml in deionized water, Sigma Chemical) mounted with Prolong antifade mounting medium (Molecular Probes, Eugene, OR), and imaged or were processed for indirect immunofluorescence (see below).

Florescence signals were visualized under an epifluorescence Nikon T2000 microscope (Melville, NY) to localize DAPI and Cy3 labeling under 100× magnification. Fluorescent images were captured with a Spot Cam (Diagnostic Instruments, Avon, MA). Integration times typically ranged between 400–800 ms for Cy3 capture and 50–100 ms for DAPI. At the beginning of each session optimum exposure times were determined and held constant throughout so that all cells experienced identical exposures. In all cases telomeric signals were within the linear response range, confirmed by the use of fluorescent microbead intensity standards (Inspeck, Molecular Probes). Photobleaching of the cy3 probe was linear <5% per 1000-ms exposure. Quantitation of the digitized telomere signals used an algorithm within the IP Lab Scanalytics image analysis software package (Fairfax, VA) as described by Meeker *et al.* (2002). Briefly, for a given nucleus the raw Cy3 image was filtered with a Gaussian filter after background subtraction, and the corrected image segmented on gray-value thresholding for contouring of telomeric spots that were then binarized to create a mask. Telomeric signals identified by the mask that were larger than background and contained within the DAPI-labeled area were tabulated and compared with the DAPI signal. A minimum of 250 telomeres were measure for each condition.

Real-Time PCR of Telomeric DNA

Genomic DNA was isolated from P19 cells and serial dilutions (10–0.625 ng/μl) from each stage of differentiation (see *Results*) were amplified by real-time PCR on a Perkin-Elmer Cetus machine (Norwalk, CT) using SYBR green to detect increases in double-stranded DNA to determine relative telomere amounts as described previously (Cawthon, 2002; Gil and Coetzer, 2004) with the following modifications to the primers: Tel-1: 5′-CGG-TTT-GTT-TGG-GTT-TGG-GTT-TGG-GTT-TGG-GTT-TGG-GTT-3′; TEL-2: 5′-GGC-TTG-CCT-TAC-CCT-TAC-CCT-TAC-CCT-TAC-CCT-TAC-CCT-3′. The method amplifies telomeric DNA 80–500 base pairs in length. The relative amounts of telomere DNA under each of the differentiation conditions was calculated from the threshold of amplification (Ct) value using the ΔΔ method using the formula: 10^((average Ct (sample) − Ct y intercept)/slope).

Telomerase Repeat Amplification Protocol Assay

Telomerase activity was measured by using a real- time PCR assay that measures the ability of telomerase to extend an exogenous primer (Wege *et al.,* 2003, Herbert *et al.,* 2006). Briefly, P19 cells were lysed at 4°C in 10 mM Tris buffer containing 0.5% CHAPS, 1 mM AEBSF, RNAse inhibitor, and BME. The following primers were used to amplify serial dilutions of 1, 0.1, 0.01, and 0.001 μg/μl protein: Forward (TS): 5′AATCCGTCGAGCAGAGTT3′; Reverse (ACX): 5′ GCGCGGCTTACCCTTACCC-TTACCCTAACC 3′ on a Perkin Elmer-Cetus machine using either Cy5 or SYBR green to detect increases in double-stranded DNA. RNAse and heat controls were included to confirm that the activity is due to the telomerase holoenzyme and not to nonspecific amplification (Kim and Wu, 1997).

Generation of ES and P19 Lines Stably Expressing Mouse Telomerase

The mouse telomerase (mTERT) gene was excised from the PGRN188 vector and cloned into the EcoRI site of the pBABE PURO retrovirus. Correct orientation of the insert was verified with SalI and XhoI. Both mTERT/pBABEpuro and empty vector DNA were transfected into Phoenix E packaging cells and viral particles, collected 48 h later, and used to infect either mouse D3 ES or P19 EC cells. Cells in which the virus had stably integrated were selected in 2 μg/ml puromycin and maintained in 1 μg/ml puromycin. Six independent clonal lines expressing mTERT in ES cells (M1-6) and in P19 cells (A1-6) and three independent lines expressing empty vector (ESC1-3 or P1-3) were selected for analysis from a total of >50 produced in each cell line.

Differentiation of ES and P19 Embryonal Carcinoma Cells

D3ES cells were maintained in DMEM with 15% FBS, 1 × NEAA, 1× L-glutamine, 0.1 mM β-mercaptoethanol, and 1200 U/ml ESGRO (Invitrogen, Carlsbad, CA). Neuroectodermal differentiation was induced by reducing FBS to 10% and removing ESGRO for 2 d and then adding 1 μM RA for 4 more days before changing medium to DMEM/F12 with 1 × N2, 1 μg/ml laminin, and 10 ng/ml basic fibroblast growth factor (bFGF) for 4 d. Neural differentiation was completed by changing media to Neurobasal medium with 4 mM L-glutamine, 1 × N2, 1 × B27, and 1 μg/ml laminin and plating cells at 1 × 10^4/well in four-well Labtek plates coated with 30 μg/ml polyornithine and 5 μg/ml laminin for a further 7 d (Bain *et al.,* 1995). P19 EC cells were maintained in α-MEM with 7.5% newborn calf serum and 2.5% fetal bovine serum. Neuroectodermal differentiation of P19 cells was induced with 0.5 μM RA and plating onto nonadherent bacterial Petri dishes. Medium and RA was replenished after 48 h, and cells were plated onto tissue culture plastic after 2 more days to complete differentiation (Jones-Villeneuve *et al.,* 1983).

Immunoreactivity of Differentiating Cells

Telomeres were detected in fixed cells using a cy3-labeled PNA probe (Molenaar *et al.,* 2003). For concurrent immunocytochemistry Formalin-fixed cells were labeled with Nestin antibody 401 (Developmental Studies Hybridoma Bank), followed by a fluoroesceinated secondary antibody and nuclei counterstained with DAPI. To determine when Nestin is up-regulated, the percentage of total cells expressing Nestin at each day after RA treatment was quantitated as follows: five fields of cells from each of two slides from two independent differentiations were photographed at 20 × magnification using a Spot digital camera connected to a Nikon fluorescent microscope. Approximately 100 DAPI-labeled nuclei were counted in each field and the numbers of cells also labeled with Nestin was determined. To investigate neuronal differentiation, 5- or 6-d cultures on adherent substrates were fixed with 4% PFA and labeled with βIII-tubulin antibody (TuJ-I, Covance, Madison, WI), a marker for mature neurons. Immunoreactivity was visualized with a fluorescent secondary antibody, and nuclei were counterstained with DAPI.

S phase Labeling with Halogenated Nucleotides

RA-treated ES and EC cells were incubated for 1 h at 37°C in 20 μM bromodeoxyuridine (BrdU). EC cells were further treated with 100 μM chlorodeoxyuridine (ClDU) for 16 h followed by 100 μM iododeoxyuridine (IDU) for 2 h (Alexiades and Cepko, 1996; Takahashi *et al.,* 1996; Shen *et al.,* 2004) and then fixed in 5% acetic acid in methanol for 12 min at 20°C. To detect labeling of cells in S phase, DNA in fixed cells was denatured with 4 N HCl, and neutralized, and then cells were incubated with specific anti-BrdU antibodies (Dolbeare and Selden, 1994). BrdU antibodies were from Becton Dickinson (Mountain View, CA); ClDU and IDU labeling was detected via anti BrdU antibodies that cross react with ClDU or IDU only, i.e., ClDU with MAS 250c (Harlan-Sera Lab, Loughborough, England), and IDU with B44 (Becton Dickinson; Aten *et al.,* 1994).

RESULTS

Reduction in Telomere Length during Neuronal Differentiation

The initial stages of neuroectodermal differentiation in P19 cells are highly reproducible because RA treatment synchronizes the cell population (Ninomiya *et al.,* 1997). Markers of neuronal precursors (Nestin, RC1, and A2B5) are significantly up-regulated at the third cell cycle after 2 d, and neural differentiation is complete within 6–8 d (Figure 1A, Shen *et al.,* 2004). In contrast, initiating primary ES cell differentiation does not synchronize the population, and neural differentiation takes >20 d to complete (Figure 1A, e.g., Bain *et al.,* 1995). In P19s, the amount of telomeric DNA at the third cycle, detected by real-time PCR (Cawthon, 2002; Gil and Coetzer, 2004), decreased by 14.7-fold compared with undifferentiated cells (Supplementary Table 1). To verify this result telomere length was further quantitated by hybridizing telomeres in fixed cells with a cy3-labeled PNA probe (Q-FISH; see *Materials and Methods*) or by hybridizing Southern blotted telomere DNA to a digoxigenin-labeled probe (TAGGG assay; see *Materials and Methods*). In each case a dramatic reduction in telomere length was detected: Densitometry of hybridized PNA probe revealed an average decline of sixfold from 195 ± 34.19–32 ± 8.0 (fluorescence units, Figure 1C), whereas the TAGGG assay revealed an average decline in telomere length of 10.5-fold from 42 to 4 kb (Figure 1B–D). In contrast telomere length recovered by 5 d to 0.6-fold compared with undifferentiated cells by Q-PCR, 0.54-fold by Q-FISH analysis or 0.46-fold by the Southern assay. Thus each method consistently reports a catastrophic decrease and recovery in telomere amount that is reflected in changes in length, even though the quantitated amount differs reflecting differences in the assay systems. Double-labeling PNA-hybridized cells with antibodies against Nestin, a marker of neural stem cells/precursors that represent ~50% of the population at this time point (Shen *et al.,* 2004, and refer to Figure 4), showed that at 48 h Nestin-expressing cells had undetectable telomeres (Figure 2A).

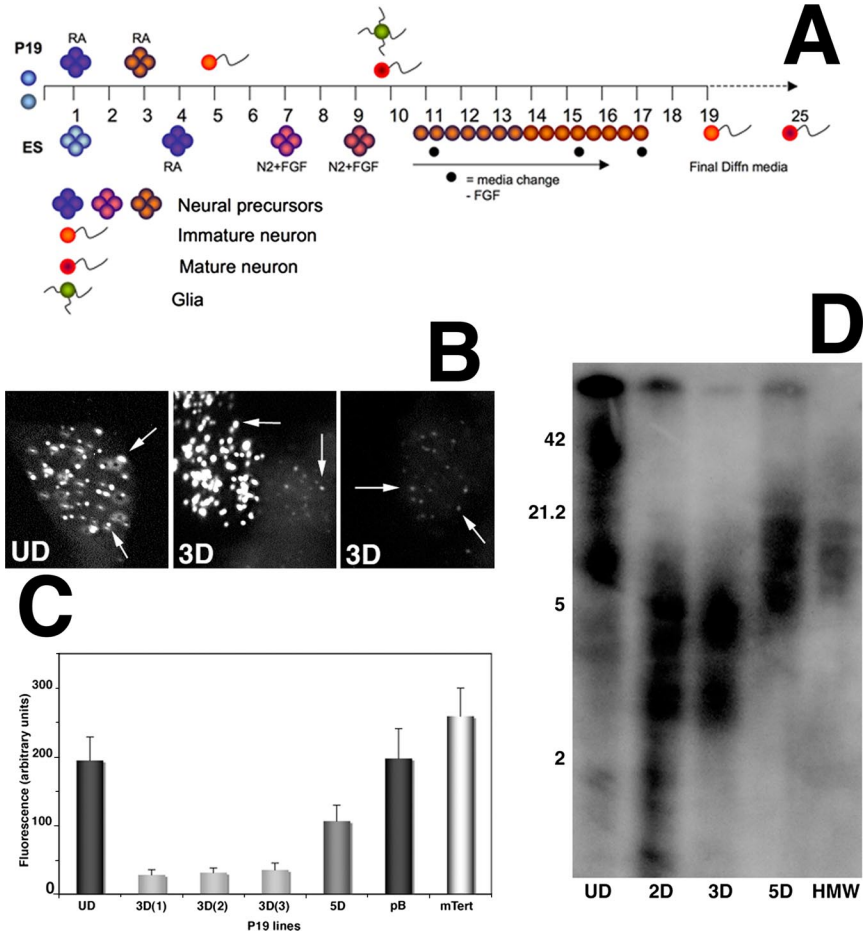

Figure 1. Regulation of telomeric DNA in differentiating P19 cells. (A) Stages in the neuroectodermal differentiation of P19 EC cells (above the time line) and D3 ES cells (below the time line). In both cases differentiation is initiated with retinoic acid (RA) and forced aggregation. In the absence of FGF-2 mTERT expressing P19 cells deaggregate and undergo apoptosis at day 3. ES cells are normally cultured with FGF-2. When FGF-2 is removed at day 18, mTERT-expressing cells undergo apoptosis. (B) Fluorescence photomicrographs of P19s either undifferentiated (left panel) or 3 d after treatment with RA to initiate differentiation that have been hybridized to the cy3-labled PNA probe. Middle panel, two cells, only one of which strongly hybridized to the probe; right panel, a cell in which hybridization has decreased. (C) Quantitation of PNA hybridization in P19 cells either undifferentiated (UD) or after 3 and 5 d (3D, 5D). Undifferentiated P19s transfected with control vector (PB) or mTERT provided for comparison. (D) Southern blot of P19 DNA that has been hybridized to a digoxigenin-labeled telomere probe showing decrease in actual telomere length after RA treatment that recovers by 5 d. HMW, high-molecular-weight telomere control.

Those cells that did hybridize strongly constituted <5% of the total, suggesting that they represent the non-RA-responsive cohort. In contrast only 12 h earlier, at 36 h after RA treatment, a significant population of cells beginning to acquire Nestin immunoreactivity still hybridized to the PNA probe (Figure 2B). Likewise, in ES cells 5 d after RA treatment to initiate neural differentiation, the PNA probe hybridized most strongly to cells that did not express Nestin (Figure 2C), whereas 48 h earlier no such difference in labeling was apparent. Hence in P19s a catastrophic loss of telomeric DNA in neural precursors occurs within merely three cell cycles after RA treatment as the cells initiate neuroectodermal differentiation. In P19s after 5 d, when the relative amount of telomere DNA in the total population recovered to ~0.6 of that in undifferentiated cells, the PNA probe hybridized strongly to a few spots in the nucleus, indicating significant differences in telomere length between individual chromosomes (Figure 2D). The reduction in telomeric DNA at the onset of differentiation did not correlate with a corresponding reduction in TERT activity: Serial dilutions of protein from the same samples used to determine relative telomere amounts were analyzed using the PCR-based telomere repeat amplification (TRAP) method (Wege *et al.*, 2003; Herbert *et al.*, 2006). At the dilution equivalent to 1 cell (0.001 $\mu g/\mu l$) there was no significant difference in the threshold cycle (Ct) for amplification in each of the three conditions (undifferentiated, Ct = 32.89; 48 h after RA, Ct = 32.46; 5 d after RA, Ct = 34.41). Hence TERT activity does not change during the third to fourth cell cycles when catastrophic loss of telomeric DNA occurs.

Table 1. Summary of threshold cycle data for telomere amplification using Q-PCR

Ct	Telomere	GAP-43
UD	18.24 ± 0.18 (0.9865)	32.74 ± 0.5 (0.8533)
3 day	22 ± 0.22 (0.9795)***	33.08 ± 0.27 (0.8945)
6 day	18.49 ± 0.21 (0.9674)	33.02 ± 0.2 (0.9243)

The threshold cycle (Ct) was determined at the Y intercept for each of the samples. The relative amounts of telomeric DNA in each sample was calculated by DΔ (see *Materials and Methods*) and averaged, with R^2 values in parentheses. Levels at the third cell cycle were decreased by 14.7-fold and at differentiation by 0.66-fold, compared with undifferentiated cells. The difference between the Cts for partially differentiated telomeric DNA and the other samples was significant (***$p < 0.001$) by ANOVA analysis followed by Student's *t* test. (n = 3 independent experiments).

Generation and Functional Characterization of P19 and ES Lines Stably Overexpressing the mTERT Gene

To determine whether either P19 or ES cells overexpressing telomerase would initiate neuroectodermal differentiation normally, the mTERT gene (a generous gift of Dr. Ronald DePinho, Dana Farber Cancer Institute, Boston, MA) was cloned into the pBABEpuro vector (a generous gift of Dr.

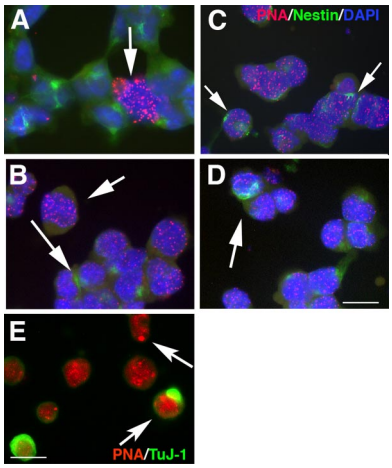

Figure 2. PNA Probe labeling of telomeres in diffderentiating P19 and ES cells. (A–D) Fluorescent photomicrographs of P19 cells and ES cells hybridized to a cy3-labeled PNA probe that reacts with telomeric DNA (Applied Biosystems) and mAb 401 against Nestin (DSHB). Nuclei were labeled with DAPI. (A and B), 48 h after RA treatment. (A) In P19 cells hybridization with the PNA probe is confined to non-nestin-expressing cells (arrow) and is absent, or restricted to only one or two spots, in nestin expressing cells. (B) In ES cells hybridization is more robust in non-nestin–expressing cells (short arrow) than in cells expressing nestin (long arrow). (C and D) Four days after RA treatment. In both P19 cells (C) and ES cells (D) nestin-expressing cells hybridize robustly with the PNA probe, indicating long telomeres (arrows). Bar, 25 μm. (E) P19 cells 48 h after RA treatment were also reacted with mAb TuJ-1 against βIII tubulin. Arrows show intense labeling of specific telomeres in some cells. Bar, 25 μm.

Robert Weinberg, Massachusetts Institute of Technology, Cambridge, MA), and virus particles obtained by infection of Phoenix E cells with the plasmid were used to infect undifferentiated P19 cells (see *Materials and Methods*). Six independent puromycin-resistant P19 and ES clones stably expressing mTERT and three independent P19 and ES lines stably expressing pBABEpuro were selected.

Insertion of mTERT and pBABE into the P19 genome was verified by PCR as described (Rahman *et al.*, 2005) except that the following reverse primer was used for mTERT: 5′-GCA GGACACCTGGCGGAAGGA-3′ (R. Rahman, personal communication; Figure 3A). Overexpression of mTERT protein was verified by immunocytochemistry using mTERT antibody (Figure 3B). Telomerase immunoreactivity was more intense in cells stably expressing mTERT than in those expressing only pBABEpuro. In both EC and ES cells immunoreactivity colocalized with nuclear DNA that had been labeled with DAPI. However, telomerase-containing nuclear inclusions (Figure 3B, arrows) were seen only in the mTERT-expressing cells. Similarly, telomerase immunoreactivity was also only abundant in the cytoplasm of mTERT-expressing cells (Figure 3B, right panels).

The functional consequences of mTERT overexpression on telomeres were detected in two ways: First, the TRAP assay showed a 2.5–5-fold increase in telomerase activity in the mTERT expressing undifferentiated cells compared with both wild-type cells and cells expressing vector alone. Moreover, telomerase activity did not change significantly during differentiation (results not shown). Specificity of the TRAP amplification was established with RNAse and heat controls (Kim and Wu, 1997). Second, telomere length was evaluated directly with the PNA telomere probe as before (Figure 3D). All cells hybridized with the PNA probe. However, more mTERT-expressing cells had higher levels of fluorescence even after differentiation was initiated compared with vector-expressing cells under the same conditions, suggesting that overexpressing mTERT has also caused an overall increase in telomere length in the undifferentiated EC and ES cells.

Outcomes of Neuroectodermal Differentiation in mTERT-expressing P19 and ES Lines

mTERT-expressing Cells Up-Regulate Markers of Immature Neural Progenitors Normally. Nestin is an intermediate filament protein whose up-regulation coincides with the transition between pluripotency and commitment to a neuroectodermal lineage and is therefore used to track progress of neuronal differentiation (Mani *et al.*, 2001). Immunoreactivity in the differentiating cells appears as a "perinuclear rosette" (Figure 4, A–D). All lines of differentiating P19 cells up-regulated Nestin by 2 d after RA treatment (Figure 4, A and B). Differentiating ES cells also up-regulated Nestin 2 d after RA was introduced to the culture medium (Figure 4, C and D). We quantitated up-regulation in the aggregated cells throughout the course of differentiation using DAPI-labeled nuclei to identify total cells as before (Shen *et al.*, 2004). Maximal expression (50%) of Nestin in parent or vector control P19 cells occurred 72 h after RA, whereas in mTERT-expressing lines the maximal increase was delayed to days 3–4, by which time there were no significant differences in the proportion of total cells expressing Nestin. In contrast maximal expression in parent and control ES cells occurred between days 5–7 (48–72 h after RA treatment), and the mTERT-expressing cells showed no delay. Hence mTERT-expressing P19s and ES cells make the transition between multipotent stem cell equivalents and neuronally committed stem cells in a timely manner.

mTERT-expressing P19 Cells Retain Markers of Neuroepithelial Precursors. Vimentin is an intermediate filament protein expressed in precursors of CNS neurons that acquire the neuroepithelial phenotype. During normal P19 differentiation, vimentin up-regulation is transient and spans the transition between precursors that label with Nestin and neurons that label with βIII-tubulin (Falconer *et al.*, 1989, Shen *et al.*, 2004). Hence, at day 2, all vimentin-labeled cells are also labeled with Nestin, whereas at day 4 half of the vimentin-labeled cells also label with βIII-tubulin. Vimentin up-regulation was slightly delayed in both control and mTERT-expressing lines compared with parent P19 cells (Figure 5, A and B). Moreover the proportion of cells labeling with vimentin were significantly different between control and mTERT-expressing lines. At day 4 an average of 7.8% of total cells in control lines expressed vimentin (Figure 5A) compared with an average of 70% in mTERT-expressing lines. This rose to 83% by day 6 (Figure 5B). Thus, the mTERT-expressing cells retain markers of neuroepithelial precursors. In contrast vimentin expression could not be detected in the D3 line of mouse ES cells at any stage after initiation of differentiation (not shown).

mTERT-expressing P19 cells Do Not Complete Neuronal Differentiation. The βIII-tubulin isoform is a marker of maturing neurons. During normal P19 differentiation, vimentin expressing cells begin to acquire βIII-tubulin immunoreactivity by day 3, and in cultures treated with cytosine arabinoside (AraC) to suppress cell proliferation >90% of total cells may express βIII tubulin by day 5 (Jones-Villeneuve *et al.*, 1983). In the absence of AraC 50–60% of total cells are neurons, with the remainder glial precursors (Shen *et al.*, 2004). βIII-tubulin–labeled cells were numerous in aggre-

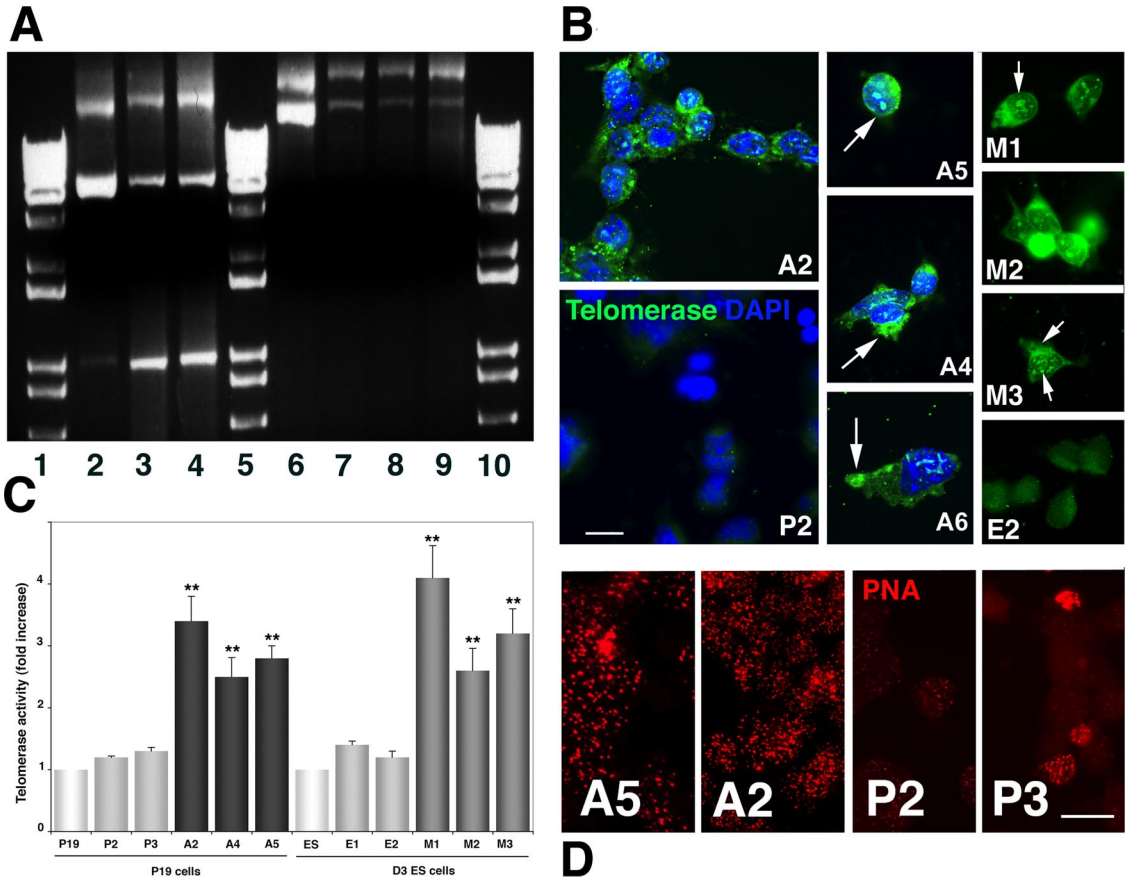

Figure 3. mTERT overexpression in P19 cells. (A) PCR amplification of pBABE puro and PBABEpuro (mTERT). Lanes 2–4, pBABE puro DNA. (2) Plasmid DNA. (3 and 4) genomic DNA from lines P2 and P3. Lanes 6–9, PBABEpuro (mTERT) DNA. (6) Plasmid DNA. (7–9) Genomic DNA from lines A2, A5, and A6. Lanes 1, 5, and 10, 1-kb ladder. (B) mTERT immunocytochemistry. Fluorescent photomicrographs of undifferentiated P19 and ES cells reacted with telomerase antibody. Nuclei were counterstained with DAPI. P19 lines (A2, A4, A5, and A6) and ES lines (M1, M2 and M3) expressing mTERT all displayed immunoreactivity in both the nucleus and cytoplasm (arrows in right panels), whereas P19 and ES cells expressing only empty vector (P2, E2) displayed little immunoreactivity. Bar, 25 μm. (C) PCR-based TRAP assay of telomerase activity performed on 100 ng extract from undifferentiated P19 and ES cells (white bars), the PBABEpuro-expressing P19 and ES lines P2, P3 and E1, E2 (light gray bars), and the PBABEpuro(mTERT)-expressing P19 lines A2, A4, and A5 (black bars) and ES lines M1, M2 and M3 (dark gray bars). Telomerase activity was significantly higher in the mTERT expressing lines than in the control or parent lines or (**$p < 0.01$) after ANOVA followed by Student's t test. Bar, 25 μm. (D) Hybridization to PNA probe: fluorescent photomicrographs of cells from the PBABEpuro(mTERT)-expressing lines A5 and A2 and the PBABEpuro-expressing lines P2 and P3 were hybridized with the cy3-labeled PNA probe. Hybridization was overall more intense in cells expressing exogenous mTERT, even at day 2 (A2) when hybridization was lower in most control cells (P3). ES cells were similar (not shown). Bar, (A2, A5) 25 μm; (P2, P3) 50 μm.

gates from the control lines but sparse in the mTERT-expressing lines at day 4 (Figure 6A). At day 5, when terminal differentiation of neurons is almost complete, ~50% of total cells in P19 parents and P2 and P3 controls expressed βIII-tubulin, whereas no more than 12% of the mTERT-expressing lines A2 and A5 expressed βIII-tubulin antibody nor did they extend neurites. Thus, the mTERT-expressing P19 neuroepithelial precursors do not complete neuronal differentiation. In contrast, βIII-tubulin was up-regulated in ~35% of cells from both ES cells and mTERT-expressing lines by day 9 of differentiation (6 d after RA treatment; Figure 5D) however only 10% of cells expressed βIII-tubulin by day 12, the remainder having died at the time that the cells were dissociated from the aggregates.

mTERT-expressing P19 and ES Cells Continue to Proliferate When Control Cells Have Ceased. BrdU, a halogenated nucleotide that intercalates in the replicating DNA of cells in S phase (Dolbeare and Selden, 1994) was used to determine the labeling index (LI) of the cells as they differentiated (Figure 7A). During normal P19 differentiation the LI begins to decrease by day 4 as symmetric cell division segues into terminal differentiation of neurons (Ninomiya *et al.*, 1997). Thus in the parent P19s and the P2 and P3 control lines, ~70% of total cells were labeled by a 6-h pulse of BrdU at day 1, when the cells are maximally synchronized (Figure 7A). By day 4 this decreased to ~25%, reflecting the cell cycle exit of terminally differentiating neurons, whereas the LI of the mTERT-expressing P19 lines remained constant at ~55%. In contrast, because ES cell differentiation is less rigorously synchronized, the time frame at which proliferation ceases cannot be specifically identified in the same way. Nonetheless, more mTERT-transfected ES cells remained in the cell cycle even after terminal differentiation of neurons had been initiated (not shown see below).

mTERT Overexpression Protects P19 Cells from Apoptosis

In P19s neuroectodermal differentiation is induced by treating cells with RA and concurrently plating them onto non-

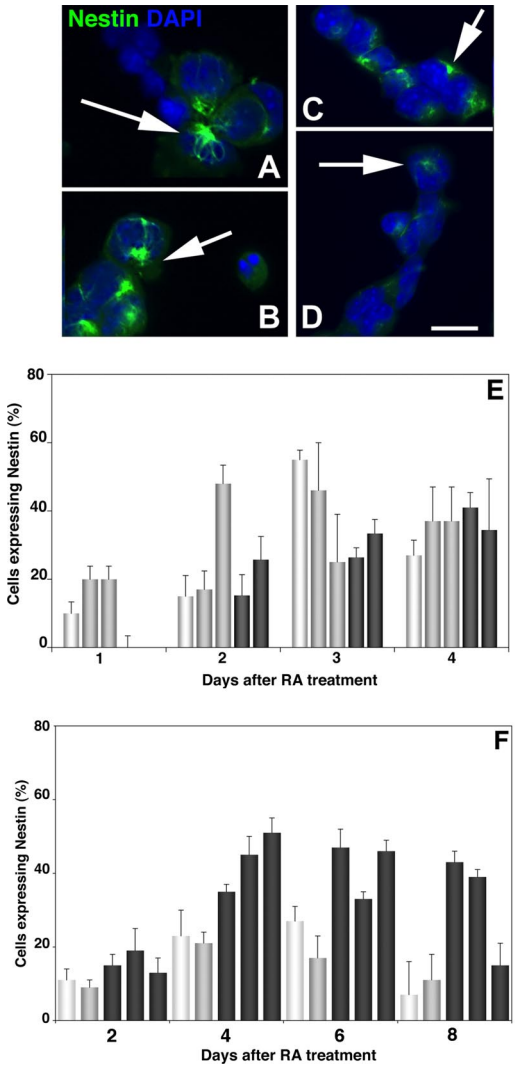

Figure 4. Upregulation of Nestin immunoreactivity in differentiating P19 and ES lines. (A–D) Fluorescent photomicrographs of mTERT-expressing P19 and ES lines 3 d after RA treatment reacted with anti-Nestin mAb. Nuclei were counterstained with DAPI. (A and B) mTERT-expressing P19 lines A4 and A5. (C and D) mTERT-expressing ES lines M1 and M3. Arrows point to "perinuclear rosette" staining characteristic of differentiating cells. Bar, 40 μm. (E) The percentage of total (DAPI-labeled) cells expressing Nestin was counted after RA treatment in P19 lines (E) and ES cells (F). Parent cells (white bars) the control lines P2 and P3 and E1 and E2 (gray bars) and the mTERT-expressing lines A4 and A5 and M1, M2, and M3 (dark gray bars). Both mTERT expressing P19s and ES cells up-regulated Nestin in a timely manner. Parent P19s up-regulated Nestin earlier, at 2 d, and by day 4 there was no significant difference in the percent of P19 cells expressing Nestin. MTERT expressing ES cells up-regulated nestin more efficiently than parent or control lines.

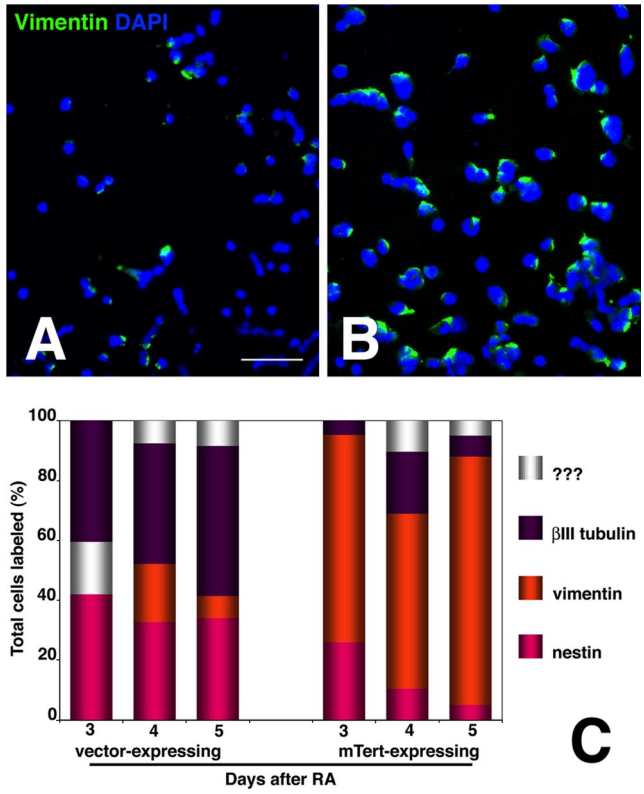

Figure 5. Persistence of vimentin immunoreactivity in differentiating mTERT-expressing lines. (A and B) Low power fluorescent photomicrographs of transfected P19 lines 3 d after RA treatment that have been reacted with anti-vimentin mAb. Nuclei were counterstained with DAPI. (A) Control line P2 (line P3 appeared similar); (B) mTERT-expressing line A5 (line A6 appeared similar). The mTERT-expressing lines show significantly more vimentin labeling. Bar 250 μm. (E) The percentage of total (DAPI-labeled) cells expressing vimentin in the control and mTERT expressing lines was averaged on days 3–5 after RA (orange) and then plotted in comparison with Nestin (pink), βIII-tubulin (purple), and non-RA responsive (white). Significantly, more cells from the mTERT-expressing lines labeled with vimentin, and those cells retained label past the time when neurons normally mature.

adherent Petri dishes, causing the cells to aggregate tightly into "embryoid-like bodies." (Treating with RA without forcing aggregation induces endothelial differentiation). Hence the proliferation of neuronal precursors is reflected in increased protein in the aggregates through day 4, at which point neuronal precursors initiate terminal differentiation, with the result that cell numbers, and protein levels stabilize (Ninomiya *et al.*, 1997). Both P19 parent and control lines behaved similarly: Cells aggregated tightly, protein levels in the aggregates increased rapidly. In P19s protein stabilized through day 5, at which point the aggregates were dissociated, and cells plated out to complete neuronal differentiation (Figure 8A). Protein levels in the mTERT-expressing aggregates also increased through day 2, but declined precipitously by day 3. Examining live cultures between days 2.0–3.0 (Figure 8, B and C) revealed that the mTERT-expressing aggregates were less well compacted than controls and that cells rapidly dissociated from them over the 12-h period between day 2.0 and day 2.5, so there was no net increase of protein in the aggregates compared with day 1. In fact, all cells in the mTERT-expressing line A2 (that showed the highest levels of mTERT activity) dissociated, preventing its use in the characterization experiments described above.

In ES cells, induction of aggregation at day 1 precedes RA treatment at day 3. All ES lines behaved similarly: proliferation of neuronal precursors was reflected in increased protein in the aggregates through day 4 after RA treatment (day 7 after initiation of differentiation), at which point the aggregates were dissociated, and cells were plated out onto laminin to complete differentiation.

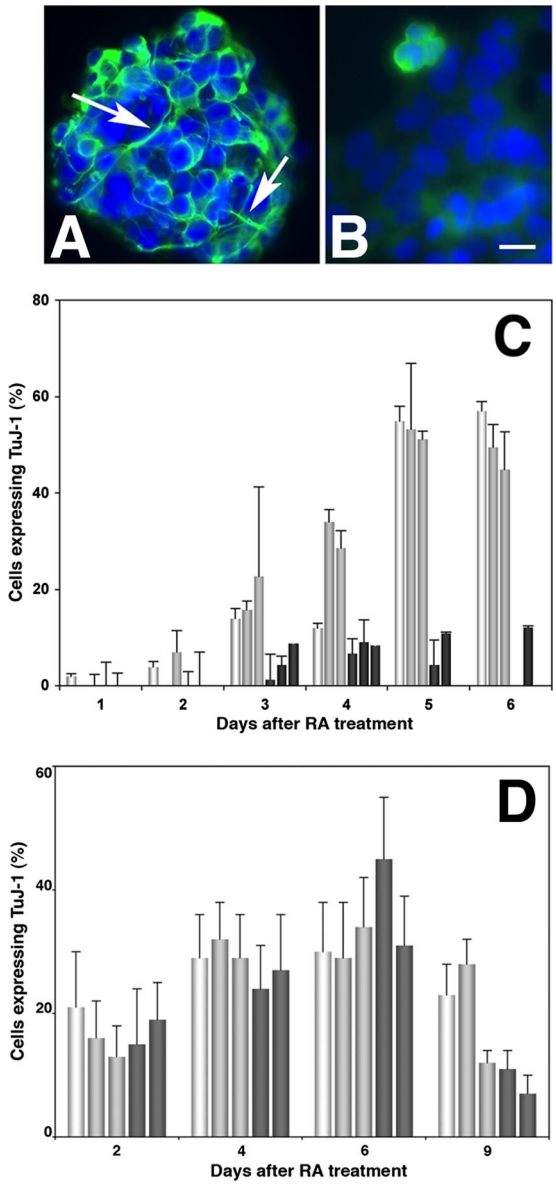

Figure 6. Differences in βIII-tubulin immunoreactivity in differentiating mTERT-expressing P19 and ES lines. (A and B) Fluorescent photomicrographs showing P19 lines 3 d after RA treatment that have been reacted with the βIII-tubulin mAb TuJ-1 followed by FITC-conjugated secondary antibody. (A) Control line P2 (line P3 appeared similar) showing intense TuJ-1 labeling in the cell body and in neurites already extended even though the cells were in aggregates (arrows). (B) mTERT-expressing line A5 (line A6 appeared similar). TuJ-1 immunoreactivity was sparse and in those cells that were labeled appeared diffuse. No neurites were seen. Bar, 25 μm. (C and D) The percentage of total (DAPI-labeled) cells expressing βIII-tubulin was counted after RA treatment in P19s (C) and ES cells (D) in parent cells (white bars), control lines (light gray bars), and the mTERT-expressing lines (dark gray bars). (C) Although 60% of parent P19s and control P2 and P3 lines and expressed βIII-tubulin by day 4, fewer than 10% of mTERT expressing lines A 4 and A5 did so, indicating that they had not completed differentiation (**$p < 0.01$ after ANOVA analysis followed by Student's *t* test). (D) In contrast there were no significant differences between control and mTERT-expressing ES lines in βIII-tubulin expression.

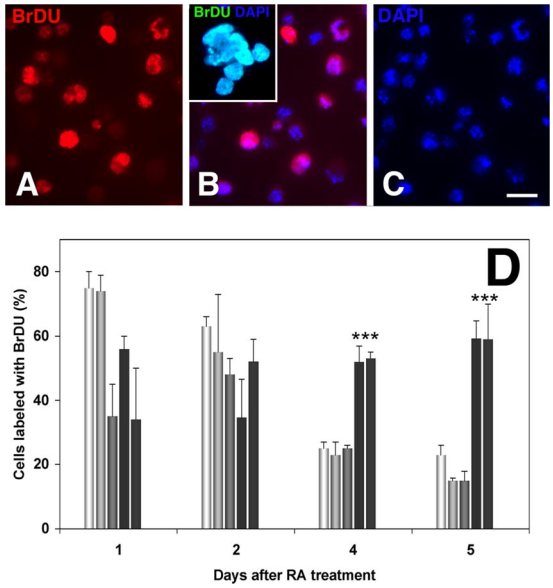

Figure 7. Enhanced BrdU incorporation in differentiating mTERT-expressing lines. (A–C) BrdU labeling of DNA 2 d after RA. P2 P19 cells were treated for 6 h with 20 μM BrdU and then fixed and reacted with an anti-BrdU antibody (Becton Dickinson). Nuclei were counterstained with DAPI. (B) Merge. Inset is merge of anti-BrdU with DAPI labeling in ES line E2. (D) The labeling index (LI): total (DAPI-labeled) cells labeled with BRDU (LI) on days 1- 5 after RA treatment; calculated P19s. Parent cells (white bar) control lines P2 and P3 (gray bars) and mTERT-expressing lines A4 and A5 (black bars). Although 70% of parent P19s and control P2 and P3 lines were in S phase at day 1, fewer than 20% were still dividing by day 5. In contrast, almost 60% of the mTERT-expressing lines remained in S phase. (***$p < 0.001$ after ANOVA analysis followed by Student's *t* test).

By 2 d after RA treatment (day 5) both differentiating control and mTERT-expressing aggregates formed blasto-cyst-like bilayered structures with an inner cell mass composed of primitive neuronal progenitors and an outer layer of nonneuronal cells (Figure 8, D–F). This inner mass increased in size through day 9 after RA (Figure 8, G–I). Unlike P19s, ES cells did not deaggregate and if maintained in suspension culture were viable and increased in size for >5 mo, past 70 population doublings (Figure 8J). When these aggregates were plated onto permissive substrates they were able to complete differentiation, but not into neurons (Figure 8K and see below).

It was not clear whether the mTERT-expressing P19 cells that remained aggregated were dying disproportionately or whether their proliferation rates slowed significantly. P19 cells undergo two characteristic apoptotic events during neuronal differentiation: the first at ~48 h after RA treatment is associated with onset of neuronal differentiation and the second between days 5–6 is associated with onset of glial differentiation (Shen *et al.*, 2004). We used the terminal deoxynucleotidyl transferase-mediated dUTP nick-end labeling (TUNEL) method to quantitate cell death in the aggregates directly (Figure 9, A and B). Both stages of apoptosis occurred normally in parent and control P19s. In contrast, apoptosis in the aggregated mTERT-expressing cells was inhibited by ~30% at 2.5 d. Hence, even though mTERT-expressing P19s tend to dissociate from the aggregates and die, if they can remain attached they are able to survive. Unlike P19s, mTERT-expressing ES cells showed little tendency to spontaneously disaggregate (see above). However, when they were dissociated to complete differentiation on laminin-coated

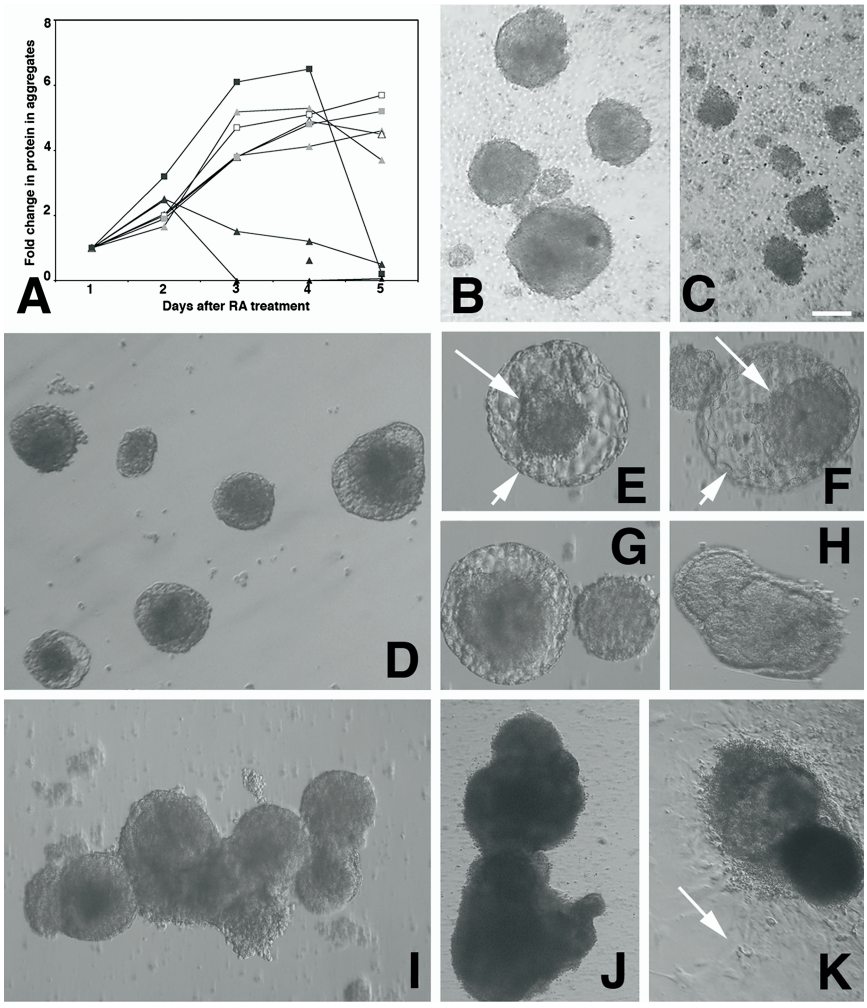

Figure 8. mTERT-expressing lines in aggregate cultures. (A) Protein content of control and mTERT-expressing aggregates during differentiation. Coomassie-based protein assays of 1 ml aliquots of aggregates from each of the lines taken from days 1–5 after RA treatment as follows: Parent P19s (open triangle); P2 & P3 control lines (grey closed triangles); mTERT expressing lines A2, A4 and A5 (black closed triangles). Note that all line A2 aggregates have dispersed by 3 days (black closed triangle), whereas the protein levels in aggregates from lines A4 and A5 has not increased from day 1. Parent ES cells (open square); E2 ES control line (grey open square); mTERT-expressing ES line M3 (black closed squares). Protein levels fall rapidly as mTERT-expressing ES lines are dissociated for plating onto laminin substrates. (B and C) Live cell images of P19 cells at 52 h after RA treatment. (B) Control line P2. (C) mTERT-expressing line A4. P19s do not form bilayered structures. mTERT-expressing aggregates are smaller and less compact and more cells have dissociated. Bar, 200 μm. (D–K) Live cell images of ES cells during neuroectodermal differentiation. (D–F) Forty-eight hours after RA treatment both parent ES (D) control (E1) line (E) and mTERT expressing line M1 (F) have formed blastocyst-like bilayered structures with an inner cell mass (small arrow) and an outer layer (large arrow). The inner mass increased; day 5 (G), day 7 (H). (I and J) ES cells maintained in suspension culture for 21 d (I) and 121 d (J). (K) Seventy-day aggregates plated onto permissive substrates. Differentiating cells migrate out from aggregates (arrow). Bar, (B–D) 200 μm; (E–G) 60 μm; (H) 200 μm; (I) 500 μm; (J) 2 mm; (K) 1 mm.

substrates, apoptosis of detached cells increased significantly compared with control or parent lines (Figure 9, C–E). Only those cells remaining tightly attached in aggregates were able to complete differentiation (Figure 9, H and I).

The results in P19s suggested that the cell cycle may have lengthened in the mTERT-expressing cells. We incubated cells at 2 d after RA with the halogenated nucleotide chlorodeoxyuridine (ClDU) and then 16 h later with iododeoxyuridine (IDU) for 2 h before fixing and staining with antibodies against BrdU that specifically cross-react with either ClDU or IDU (see *Materials and Methods*). Hence cells that remained in the cell cycle throughout would be detected as brightly labeled with both ClDU and IDU; they were detected in all lines (Figure 10, A and Bb). In contrast, cells that had exited the cell cycle during the first 16 h would label with ClDU only; they were more prevalent in control lines (Figure 10Aa). Cells having a long cell cycle would label with IDU only; they were more prevalent in the mTERT-expressing lines (Figure 10B). Finally cells that were apoptosing would have condensed nuclei. These cells were labeled with ClDU alone and were more prevalent in the control lines (Figure 10, A and Bc). Cell cycle length had increased in mTERT-expressing cells, and cells in the control lines that are targeted to die at 48 h have not re-entered the cell cycle. Because ES cells are not synchronized during early stages of differentiation, measuring cell cycle length in this manner is not feasible.

FGF Treatment Reverses Aggregate Dispersion and Increases the Proliferative Capacity of mTERT-expressing P19 Cells

In P19s overexpressing telomerase prevents aggregated cells exiting the cell cycle and dying, but cells that do not remain aggregated die immediately. Including 10 ng/ml FGF-2 together with the RA that is replenished after 48 h both reversed aggregate dispersion and prevented cell death: the volume of individual aggregates from all the cell lines increased on average five times during the first 7 d. Moreover, FGF-2–treated aggregates from each of the cell lines expressed Nestin in similar proportions to untreated cells indicating that their phenotype had not changed (not shown). Most of the cells from the FGF-treated parent and control lines died after 7 d, when differentiation would normally have been completed. In contrast cells in the mTERT-expressing aggregates continued to proliferate. After 60 d, 59 $\pm$ 5% of cells in mTERT lines expressed Nestin, whereas 37 $\pm$ 6% had gone on to express βIII tubulin. The A4 and A5 cells continued to proliferate for >5 mo in significant excess of 70 doublings, provided that FGF was included at each medium change. At 112 d after RA treatment the total protein in the mTERT-expressing aggregates was >10-fold ini-

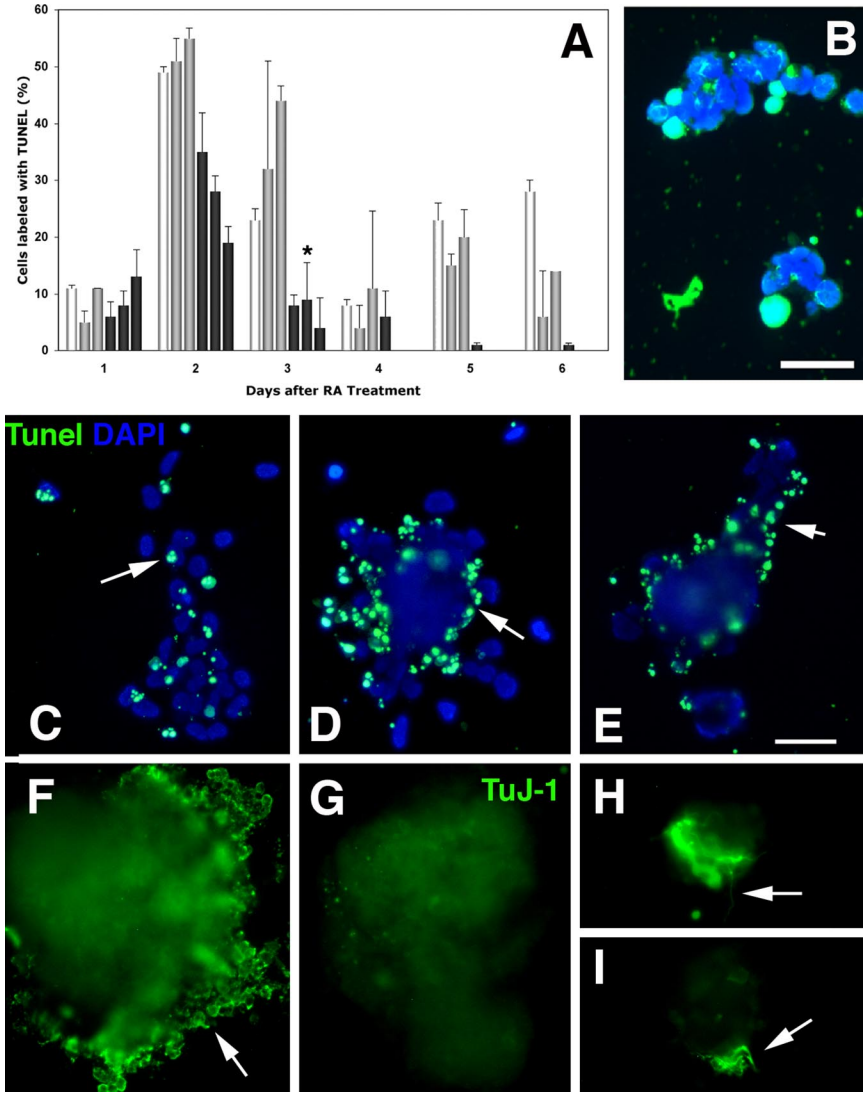

Figure 9. Fate of mTERT-expressing lines in aggregate cultures. (A) Quantitation of TUNEL labeling in aggregated cells from P19 parent cells (□) the control lines P2 and P3 (▨) and the mTERT-expressing lines A4, A5 and A2 (■). Both the parent P19s and the control lines undergo apoptotic events at days 2 and days 5 and 6, whereas apoptosis in the mTERT-expressing lines is reduced by 30%. (*$p < 0.05$ after ANOVA analysis followed by Student's t test compared with parent and P3 lines). (B) P2 cells treated with TUNEL to transfer biotin-labeled dUTP to cleaved DNA in apoptotic cells. Cell nuclei counterstained with DAPI. Bar, 50 μm. (C–I) Transfected ES cells 8 d after treatment with RA dissociated to complete differentiation. (C–E) Tunel labeling. Cell nuclei counterstained with DAPI. (C) Control line (E1), apoptotic cells are scattered throughout the aggregate (arrow). (D and E) mTERT-expressing lines M2 and M3. Apoptotic cells are concentrated at the aggregate perimeter. Bar, 500 μm. (F–H) TuJ-1 labeling to detect βIII-tubulin expression at 8 d after RA treatment. (F) ES control line E1. Cells at the perimeter of aggregates are heavily labeled with TuJ-1, indicating that they are differentiating neurons (arrow). (G–I) mTERT expressing lines M2 and M3. (G) No TuJ-1–labeled neurons migrating out from the perimeter of the M2 aggregate. (H and I) TuJ-1–labeled cells that remain within residual aggregates differentiate and send out neuritis (arrows). Bar, 500 μm.

tial levels (Figure 11A). More than 85% of the mTERT-expressing cells labeled with βIII tubulin and extended neurites, indicating that the time in culture had not selected for a nonneuronal cell population (Figure 11B). ES cells are normally cultured with FGF during the time that neural precursors proliferate and both control and mTERT-expressing cells remained aggregated and proliferated normally (see Figure 8). However if control lines were maintained in aggregates they ceased to proliferate and eventually dissociated, whereas, like P19s, mTERT-expressing lines could be maintained as proliferating aggregates at least through 5 mo after differentiation was induced. Total protein was >15-fold initial levels (Figure 11A and see also Figure 8). The aggregated cells also continued to express βIII tubulin (Figure 11C) and were able to extend neurites. However, if the aggregates were dissociated most of the Tuj-1–expressing cells died (see Figure 9), whereas nonneuronal cells survived (see Figure 8K). Hence overexpressing mTERT in both P19s and ES cells can immortalize a population of proliferating neural precursors, but whereas the P19-mTERT precursors can complete neuronal differentiation in a quantitative manner, ES-mTERT precursors are capable of differentiating into neurons, but the population does not do so quantitatively.

DISCUSSION

Here we have investigated the consequences of telomerase up-regulation on the behavior of murine neural precursors in vitro. Our results show that when either P19 embryonal carcinoma (EC) cells or D3 mouse embryonic stem (ES) cells overexpressing the rate-limiting riboprotein subunit of the telomerase enzyme, mTERT, are treated with RA to induce neuroectodermal differentiation and then are maintained aggregated in the presence of FGF, they generate a population of neural precursors with significantly enhanced proliferative potential. Our results extend the study by Roy *et al.* (2004), who transfected mTERT into ES neural progenitors themselves, by showing that differentiation can be induced normally in pluripotent cells already overexpressing telomerase and does not constitute a barrier to telomerase's ability to induce expansion of the precursor population. They also extend the study of Armstrong *et al.* (2005) who constitutively expressed mTERT in undifferentiated ES cells and showed enhanced differentiation toward the hematopoietic lineage by demonstrating that initial differentiation toward the neuroectodermal lineage is also potentiated. Like Bestilny *et al.* (1996), we also demonstrated that telomerase

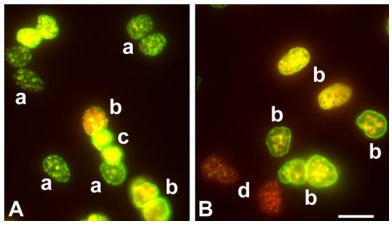

Figure 10. Cell cycle status of differentiating P19 lines. (A and B) Fluorescence photomicrographs of cells that have been incubated with 100 μM ClDU for 16 h starting 48 h after RA treatment followed by 100 μM IDU for 2 h before fixing and reacting with BrdU antibodies that specifically cross-react with either ClDU or IDU (see *Materials and Methods*). Specific ClDU labeling was visualized with FITC-conjugated secondary antibody, and specific IDU labeling was visualized with Texas Red–conjugated antibody. (A) P2 cells. (B) A4 cells. (a) Cells that incorporated ClDU at the beginning of the incubation but left the cell cycle thereafter. (b) Cells that incorporated both ClDU and IDU, indicating that they have remained in the cell cycle. (c) Cells that incorporated ClDU, having condensed nuclei indicative of apoptosis. (d) Cells that incorporated only with IDU, indicating an increased cell cycle. Bar 20 μm.

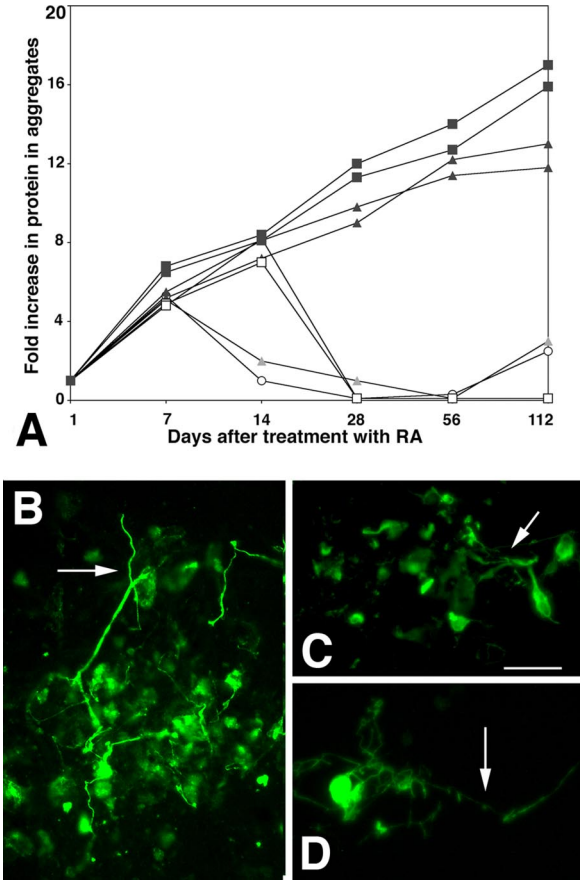

Figure 11. Long-term survival of mTERT expressing P19 and ES cells treated with FGF-2. (A) Protein concentration over time in culture in aggregated P19s and ES cells. Parent P19s (open circle) and ES cells (open square). P19 control lines P2 and P3 (grey triangles) and mTERT expressing lines M2 and M3 (black squares) that had been cultured for up to 112 days after initial treatment with RA, in the presence of 10 ng/ml FGF2. Whereas protein concentration declined rapidly in the parent and control lines, mTERT-expressing lines continued to proliferate albeit at a significantly slower rate. (B–D) mTERT expressing cells cultured for 112 d and then treated to complete differentiation before being reacted with the βIII tubulin antibody TuJ-1. B) >80% of mTERT expressing P19 cells reacted with TuJ-1 and a significant number extended neurites (arrow), indicating morphological maturation. (C and D) Very few (<5%) of mTERT-expressing ES cells reacted with TuJ-1, but those that did had neurites (arrows) indicating that they were capable of morphological maturation. Bar, 250 μm.

activity remains high in P19s as they differentiate but used three independent methods to show that even so, telomeres themselves shorten rapidly as cells acquire markers of neural precursors. In fact telomeric DNA in the differentiating cells decreases by 8–14-fold within 2 d or four cell cycles after differentiation is initiated. Such a catastrophic decrease, equivalent to a reduction in average length from 40 to <5 kb, and in association with down-regulation of either the protein or RNA component of telomerase, has been described to precede cell cycle arrest in yeast and mammalian cancer cells (Lustig, 2003, Li *et al.*, 2004, Folini *et al.*, 2005). In contrast, telomerase in the P19s remained active in the in vitro TRAP assay, implying that it cannot functionally interact with telomeric DNA in the differentiating cells. Telomerase is clearly located outside the nucleus even in cells not overexpressing mTERT (Chung *et al.*, 2005); however, the significance of this distribution as well as the mechanism causing telomeres to shorten so rapidly is not at all clear.

Overexpression of telomerase allowed us to select several independent P19 and ES lines in which both telomerase activity and telomere length were increased. The lines initiated differentiation and the neuronal precursors continued to proliferate instead of terminally differentiating. The time period during which pluripotent cells narrow their capacity as precursors while differentiating into neurons is paralleled by an important transition in how the cells handle DNA repair. In undifferentiated ES/EC cells telomerase activation is regulated by FGF-2 and TGFβ on a background of inactive p53, pRb, and E2F. In contrast differentiating ES/EC cells normally down-regulate telomerase while activating p53, pRb, and E2F, in order to be able to stimulate apoptosis if chromosomal instability occurs, thereby reducing their proliferative capacity. In P19 cells the initial apoptosis event that normally occurs in aggregated cells after 36 h (Ninomiya *et al.*, 1997) was inhibited by 30% in agreement with studies on endothelial differentiation showing that overexpressing telomerase in ES cells inhibited up-regulation of these apoptosis-pathway initiators. In fact mTERT-expressing P19 cells did not up-regulate pRb (results not shown, reviewed in Miura *et al.*, 2004).

However, telomerase overexpression is not sufficient to inhibit apoptosis in the context of an evolving phenotype: The normal process of P19 differentiation requires that cells disperse and reaggregate at 48 h when medium and RA are replenished. Most mTERT-expressing cells did not survive this manipulation, detached from the aggregates, and died. Reaggregation of P19s is a calcium/cadherin-dependent process that requires transduction of FGF-2–mediated signaling (Sakalian and Draber, 1991; Mani *et al.*, 2001). Adding FGF-2 to the replenished medium rescued the reaggregation defect and allowed the mTERT expressing cells to continue proliferating, implying that mTERT overexpression may interfere with an endogenous source of FGF-2 in the differentiating cultures. In this regard, FGF-2 has been shown to inhibit apoptosis in differentiating P19s (Miho *et al.*, 1999) as well as to regulate telomerase activity in neural precursors (Haik *et al.*, 2000) and to prevent onset of early senescence in fibroblasts (Trivier *et al.*, 2004). Together the results suggest that a FGF–telomerase positive feedback loop contributes to

the protection from the apoptotic event seen at the transition from stem cell to committed precursor. It seems likely that this involves cmyc and activity of the ets transcription factor family (reviewed by Dwyer *et al.,* 2007). In support of this notion mTERT–ES aggregates that are normally cultured in the presence of FGF-2 remained tightly aggregated and did not undergo apoptosis early in differentiation. However, removing FGF-2 and dissociating them to enable differentiation to be completed induced massive cell death, suggesting that an apoptosis inhibitor to substitute for FGF may be required. In this regard inhibition of the Rho/ROCK pathway has recently been shown to be effective in enhancing differentiation of neural precursors by inhibiting apoptosis (Koyanagi *et al.,* 2007).

In the presence of FGF-2, both types of mTERT-expressing neural precursors continued to proliferate for more than 120 d, thereby evading replicative senescence. However our results do not rule out that, as Gorbunova *et al.* (2002) showed in fibroblasts, a minor subpopulation of mTERT-expressing senescent cells do exist in the population. Protein analysis suggested that the population-doubling time had slowed significantly. In tumor cell lines, telomerase activity regulates cyclin D1 expression to enhance proliferation; in contrast, overexpression of telomerase can also cause cyclin-dependent growth inhibitors (such as p16ink4a and p21Cip1) to accumulate (Menzel *et al.,* 2006). It may be, therefore, that when telomere length itself is not rate limiting, such as in mouse cells, whether cells divide or senesce critically depends on telomerase levels and the ability to regulate the cell cycle. However, it is also clear that the telomerase levels were insufficient to recapitulate the proliferation rate of cells at the beginning of differentiation: in the ClDU/IDU double-labeling experiment many more mTERT expressing cells were labeled with IDU alone even by day 3, indicating a cell cycle length in excess of 24 h. Whether increasing telomerase activity even more, either via its protein or via its RNA component can tip the balance in favor of proliferation without enhancing tumorigenesis, remains to be seen.

The tumorigenicity of EC (and ES) cells, when transplanted into adults, has been ascribed to contamination of the transplant with residual undifferentiated or primitive precursors (Andrews *et al.,* 2005), and so it was important to establish whether long-term culture of the mTERT-expressing cells would enrich for a primitive population with tumorigenic potential. This did not appear to be the case in P19s where, after 4 mo in culture, the proportion of cells expressing precursor markers (Nestin and βIII tubulin) was significantly higher than at the beginning of the differentiation process. Whether this reflects selective apoptosis of primitive contaminants or whether they proliferate very slowly in these culture conditions is unclear, but is obviously critical because there is no acceptable level of tumorigenesis. In contrast a large population of ES cells not expressing neuronal markers survived immortalization. Whether they have been transformed also remains to be seen.

In P19s days 3–4 after RA treatment mark the transition between symmetric and asymmetric division of neuronal precursors (Shen *et al.,* 2004). The significant proportion (85%) of mTERT PI9s expressing βIII tubulin after FGF-2 treatment and long-term culture together with inhibition of apoptosis suggests that the precursors continue dividing symmetrically; otherwise there would be a higher proportion of more primitive cells in the final population. Our results imply that overexpressing telomerase inhibits the transition between symmetric and asymmetric division in P19 cells, but not their ability to complete morphological differentiation, suggesting that asymmetric cell division is not a prerequisite for neurogenesis in P19 EC cells. In contrast, there were significantly more nonneuronal cells in long-term cultures of ES cells, suggesting that telomerase activity is different. Furthermore our results showing that mTERT ES cells were not able to quantitatively complete terminal differentiation in vitro because removing FGF-2 induced apoptosis contrast with those reported by Roy *et al.* (2004) who showed functional differentiation of ES-derived telomerase expressing precursors when they were transplanted into a host in vivo. They suggest that critical extrinsic factors that inhibit apoptosis are insufficient in these in vitro conditions. The role of telomerase in neuronal differentiation has not been clear. On one hand, signals that induce cell differentiation also suppress telomerase activity, suggesting that telomerase activity decreases as a consequence of the cell differentiation (reviewed in Mattson *et al.,* 2001). On the other hand, suppressing telomerase expression with antisense (Kondo *et al.,* 1998) can induce differentiation, suggesting that it plays a functional role in the transition between proliferation and differentiation. Nonetheless, these results showing that surviving neurons can complete morphological differentiation indicate that the barrier preventing neuronal differentiation in vitro is not insurmountable in the presence of telomerase and together the results further emphasize the importance of telomerase in stem cell biology independent of its function in telomere regulation.

ACKNOWLEDGMENTS

The authors thank Alyssa Okun and Christopher Bartolome for expert technical assistance and Drs. Ronald DePinho and Bob Weinberg for their generous gifts of reagents.

REFERENCES

Alexiades, M. R., and Cepko, C. (1996). Quantitative analysis of proliferation and cell cycle length during development of the rat retina. Dev. Dyn. *205*, 293–307.

Andrews, P. W., Matin, M. M., Bahrami, A. R., Damjanov, I., Gokhale, P., and Draper, J. S. (2005). Embryonic stem (ES) cells and embryonal carcinoma (EC) cells: opposite sides of the same coin. Biochem. Soc. Trans. *33*, 1526–1530.

Armstrong, L., Lako, M., Lincoln, J., Cairns, P. M., and Hole, N. (2000). mTERT expression correlates with telomerase activity during the differentiation of murine embryonic stem cells. Mech. Dev. *97*, 109–116.

Armstrong, L., Saretzki, G., Peters, H., Wappler, I., Evans, J., Hole, N., von Zglinicki., T., and Lako, M. (2005). Overexpression of telomerase confers growth advantage, stress resistance and enhanced differentiation of ESCs toward the hematopoetic lineage. Stem Cells *23*, 516–529.

Astigiano, S., Damonte, P., Fossati, S., Boni, L., and Barbieri, O. (2005). Fate of embryonal carcinoma cells injected into postimplantation mouse embryos. Differentiation *73*, 484–490.

Aten, J. A., Stap, J., Hoebe, R., and Bakker, P. J. (1994). Application and detection of IdUrd and CldUrd as two independent cell-cycle markers. Methods Cell Biol. *41*, 317–326.

Bain, G., Kitchens, D., Yao, M., Huettner, J. E., and Gottlieb, D. I. (1995). Embryonic stem cells express neuronal properties in vitro. Dev. Biol. *168*, 342–357.

Bestilny, L. J., Brown, C. B., Miura, Y., Robertson, L. D., and Riabowol, K. T. (1996). Selective inhibition of telomerase activity during terminal differentiation of immortal cell lines. Cancer Res. *56*, 3796–3802.

Cawthon, R. M. (2002). Telomere measurement by quantitative PCR. Nucleic Acids Res. *30*, e47.

Chang, M. W., Grillari, J., Mayrhofer, C., Fortschegger, K., Allmaier, G., Marzban, G., Katinger, H., and Voglauer, R. (2005). Comparison of early passage, senescent and hTERT immortalized endothelial cells. Exp. Cell Res. *309*, 121–136.

Chung, H. K., Cheong, C., Song, J., and Lee, H. W. (2005). Extratelomeric functions of telomerase. Curr. Mol. Med. *5*, 233–241.

Dolbeare, F., and Selden, J. R. (1994). Immunochemical quantitation of bromodeoxyuridine: application to cell-cycle kinetics. Methods Cell Biol. *41*, 297–316.

Dwyer, J., Li, H., Xu, D., and Liu, J. P. (2007). Transcriptional regulation of telomerase activity: roles of the ets transcription factor family. Ann. NY Acad. Sci. *1114*, 36–47.

Emsley, J. G., Mitchell, B. D., and Kempermann, G., and Macklis, J. D. (2005). Adult neurogenesis and repair of the adult CNS with neural progenitors, precursors, and stem cells. Prog. Neurobiol. *75*, 321–341.

Falconer, M. M., Vielkind, U., and Brown, D. L. (1989). Association of acetylated microtubules, vimentin intermediate filaments, and MAP 2 during early neural differentiation in EC cell culture. Biochem. Cell Biol. *67*, 537–544.

Folini, M., Brambilla, C., Villa, R., Gandellini, P., Vignati, S., Paduano, F., Daidone, M. G., and Zaffaroni, N. (2005). Antisense oligonucleotide-mediated inhibition of hTERT, but not hTERC, induces rapid cell growth decline and apoptosis in the absence of telomere shortening in human prostate cancer cells. Eur. J. Cancer *41*, 624–634.

Gil, M. E., and Coetzer, T. L. (2004). Real-time quantitative PCR of telomere length. Mol. Biotechnol. *27*, 169–172.

Gorbunova, V., Seluanov, A., and Perreira-Smith, O. (2002). Evidence that high telomerase activity may induce a senescent-like growth arrest in human fibroblasts. J. Biol. Chem. *278*, 7692–7698.

Haik, S., Gauthier, L. R., Granotier, C., Peyrin, J. M., Lages, C. S., Dormont, D., and Boussin, F. D. (2000). Fibroblast growth factor 2 up regulates telomerase activity in neural precursor cells. Oncogene *19*, 2957–2966.

Hardy, K., Carthew, P., Handyside, A. H., and Hooper, M. L. (1990). Extragonadal teratocarcinoma derived from embryonal stem cells in chimaeric mice. J. Pathol. *160*, 71–76.

Herbert, B.-S., Hochreiter, A. E., Wright, W. E., and Shay, J. W. (2006). Non-radioactive detection of telomerase activity using the telomeric repeat amplification protocol. Nat. Protocols *1*, 1583–1590.

Jones-Villeneuve, E. M., Rudnicki, M. A., Harris, J. F., and McBurney, M. W. (1983). Retinoic acid-induced neural differentiation of embryonal carcinoma cells. Mol. Cell. Biol. *3*, 2271–2279.

Kim, N. W., and Wu, F. (1997). Advances in quantification and characterization of telomerase activity by (TRAP). Nucleic Acids Res. *13*, 2595–2597.

Kondo, S. *et al.* (1998). Antisense telomerase treatment: induction of two distinct pathways, apoptosis and differentiation. FASEB J. *12*, 801–811.

Koyanagi, M., Takahashi, J., Arakawa, Y., Doi, D., Fukuda, H., Hayashi, H., Narumiya, S., and Hashimoto, N. (2007). Inhibition of the Rho/ROCK pathway reduces apoptosis during transplantation of embryonic stem cell-derived neural precursors. J. Neurosci. Res. *Epub ahead of print*.

Li, S., Rosenberg, J. E., Donjacour, A. A., Botchkina, I. L., Hom, Y. K., Cunha, G. R., and Blackburn, E. H. (2004). Rapid inhibition of cancer cell growth induced by lentiviral delivery and expression of mutant-template telomerase RNA and anti-telomerase short-interfering RNA. Cancer Res. *64*, 4833–4840.

Lustig, A. J. (2003). Clues to catastrophic telomere loss in mammals from yeast telomere rapid deletion. Nat. Rev. Genet. *4*, 916–923.

Mani, S., Shen, Y., Schaefer, J., and Meiri, K. F. (2001). Failure to express GAP-43 during neurogenesis affects cell cycle regulation and differentiation of neural precursors and stimulates apoptosis of neurons. Mol. Cell. Neurosci. *17*, 54–66.

Mattson, M. P., Fu, W., and Zhang, P. (2001). Emerging roles for telomerase in regulating cell differentiation and survival: a neuroscientist's perspective. Mech. Aging Dev. *122*, 659–671.

McBurney, M. W. (1993). P19 embryonal carcinoma cells. Int. J. Dev. Biol. *37*, 135–140.

Meeker, A. K., Gage, W. R., Hicks, J., Simon, I., Coffman, J., Platz, E., March, G. E., and De Marzo, A. M. (2002). Telomere length assessment in human archival tissues combined telomere fluorescence in situ hybridization and immunostaining. Am. J. Pathol. *160*, 1259–1268.

Menzel, O., Migliaccio, M., Goldstein, D. R., Dahoun, S., Delorenzi, M., and Rufer, N. (2006). Mechanisms regulating the proliferative potential of human CD8+ T lymphocytes overexpressing telomerase. J. Immunol. *177*, 3657–3668.

Miho, Y., Kouroku, Y., Fujita, E., Mukasa, T., Urase, K., Kasahara, T., Isoai, A., Momoi, M. Y., and Momoi, T. (1999). bFGF inhibits the activation of caspase-3 and apoptosis of P19 embryonal carcinoma cells during neuronal differentiation. Cell Death Differ. *6*, 463–470.

Miura, T., Mattson, M. P., and Rao, M. S. (2004). Cellular lifespan and senescence signaling in embryonic stem cells. Aging Cell *3*, 333–343.

Molenaar, C., Wiesmeijer, K., Verwoerd, N. P., Khazen, S., Eils, R., Tanke, H. J., and Dirks, R. W. (2003). Visualizing telomere dynamics in living mammalian cells using PNA probes. EMBO J. *22*, 6631–6641.

Natesan, S. (2005). Telomerase extends a helping hand to progenitor cells. Trends Biotechnol. *23*, 1–3.

Ninomiya, Y., Adams, R., Morriss-Kay, G. M., and Eto, K. (1997). Apoptotic cell death in neuronal differentiation of P19 EC cells: cell death follows reentry into S phase. J. Cell. Physiol. *172*, 25–35.

Rahman, R., Latonen, L., and Wiman, K. G. (2005). hTERT antagonizes p53-induced apoptosis independently of telomerase activity. Oncogene *24*, 1320–1327.

Roy, N. S. *et al.* (2004). Telomerase immortalization of neuronally restricted progenitor cells derived from the human fetal spinal cord. Nat. Biotechnol. *22*, 297–305.

Sakalian, M., and Draber, P. (1991). Changes in surface glycoconjugates in adhesion-defective variants of P19 embryonal carcinoma cells. Int. J. Dev. Biol. *35*, 473–479.

Sarin, K. Y., Cheung, P., Gilison, D., Lee, E., Tennen, R. I., Wang, E., Artandi, M. K., Oro, A. E., and Artandi, S. E. (2005). Conditional telomerase induction causes proliferation of hair follicle stem cells. Nature *436*, 1048–1052.

Sharpless, N. E., and DePinho, R. A. (2004). Telomeres, stem cells, senescence, and cancer. J. Clin. Invest. *113*, 160–168.

Shen, Y., Mani, S., and Meiri, K. F. (2004). Failure to express GAP-43 leads to disruption of a multipotent precursor and inhibits astrocyte differentiation. Mol. Cell. Neurosci. *26*, 390–405.

Takahashi, T., Nowakowski, R. S., and Caviness, V. S., Jr. (1996). The leaving or Q fraction of the murine cerebral proliferative epithelium: a general model of neocortical neuronogenesis. J. Neurosci. *16*, 6183–6196.

Teramoto, S., Kihara-Negishi, F., Sakurai, T., Yamada, T., Hashimoto-Tamaoki, T., Tamura, S., Kohno, S., and Oikawa, T. (2005). Classification of neural differentiation-associated genes in P19 embryonal carcinoma cells by their expression patterns induced after cell aggregation and/or retinoic acid treatment. Oncol. Rep. *14*, 1231–1238.

Trivier, E., Kurz, D. J., Hong, Y., Huang, H. L., and Erusalimsky, J. D. (2004). Differential regulation of telomerase in endothelial cells by fibroblast growth factor-2 and vascular endothelial growth factor-a: association with replicative life span. Ann. NY Acad. Sci. *1019*, 111–115.

Wege, H., Chui, M. S., Le, H. T., Tran, J. M., and Zern, M. A. (2003). SYBR Green real-time telomeric repeat amplification protocol for the rapid quantification of telomerase activity. Nucleic Acids Res. *31*, E3–3.

Zeng, X., and Rao, M.S.H. (2007). Human embryonic stem cells: long term stability, absence of senescence and a potential cell source for neural replacement. Neuroscience *145*, 1348–1358.